

◆ Article type

Original article

◆ Title

Dry-gel Conversion Synthesis of Magnetic BEA-type Zeolites for Antibiotics Adsorption

◆ Authors

Vanpaseuth Phouthavong¹

Takeshi Hagio^{1,2,*}

Supinya Nijpanich³

Jae-Hyeok Park²

Masatake Hiraiwa¹

Teeranun Srihirunthanon^{4,5}

Nutchanan Chantanurak^{4,5}

Ratana Rujiravanit^{4,5}

Yuki Kamimoto⁶

Xinling Li⁷

Long Kong⁸

Liang Li⁸

Ryoichi Ichino^{1,2}

◆ Affiliation

¹ Department of Chemical Systems Engineering, Graduate School of Engineering, Nagoya University, Furo-cho, Chikusa-ku, Nagoya 464-8603, Japan

² Institute of Materials Innovation, Institutes of Innovation for Future Society, Nagoya University, Furo-cho, Chikusa-ku, Nagoya 464-8601, Japan

³ Synchrotron Light Research Institute (Public Organization), Nakhon Ratchasima 30000, Thailand

⁴ The Petroleum and Petrochemical College, Chulalongkorn University, Bangkok 10330, Thailand

⁵ Center of Excellence on Petrochemical and Materials Technology, Chulalongkorn University, Bangkok 10330, Thailand

⁶ Department of Environmental Science, Faculty of Human Environment, University of Human Environments, Okazaki 444-3505, Japan

⁷ School of Mechanical Engineering, Shanghai Jiao Tong University, 800 Dongchuan Road Shanghai 200240, China

⁸ School of Environment Science and Engineering, Shanghai Jiao Tong University, 800 Dongchuan Road Shanghai 200240, China

◆ Corresponding Author Information

Takeshi HAGIO hagio@mirai.nagoya-u.ac.jp

Highlights

- Effect of dry-gel conversion synthesis conditions for magnetic BEA zeolite composites is studied.
- Homogenous BEA zeolite/Fe₃O₄ composite was successfully synthesized using the optimal conditions.
- The composite exhibits magnetic properties and could be easily collected using a magnet.
- The obtained product could effectively remove sulfadiazine, especially from acidic solutions.
- The adsorption was found to be of a multilayer type and followed the Freundlich model.

Abstract

The dry-gel conversion method (DGC) is a promising synthesis protocol for preparing magnetic zeolite composites as it yields homogeneous composite particles with more rapid crystallization, smaller reactor volume, and less waste production than the conventional hydrothermal method. This work investigates the optimal conditions for preparing magnetic BEA-type zeolites using the DGC method, including the gel/water ratio, crystallization temperature and time. Precursor dry-gel incorporating well-dispersed magnetite was subjected to crystallization under water vapor atmosphere with a gel/water ratio of 0.5–2, crystallization temperature of 140–200 °C for 1.5–12 h, followed by characterization using X-ray diffraction and scanning electron microscopy. The optimum conditions were found to be gel/water ratio of 1 and crystallization at 180 °C for 12 h. Magnetic properties of collected samples were evaluated using a vibrating-sample magnetometer after calcination at 400–500 °C for 12 h. Products calcined below 450 °C showed good magnetic properties. Adsorption of sulfadiazine using the BEA and magnetic BEA-type zeolites was evaluated in a 10–50 mg/L range. Results revealed favorable multilayer-type adsorption of sulfadiazine onto both non-magnetic and magnetic BEA-type zeolites (Freundlich model). These indicate that DGC method is suitable for preparing high-silica magnetic BEA-type zeolites with potential for antibiotic removal.

Keywords: Dry-gel conversion; BEA-type zeolite; magnetic zeolite; antibiotic removal; sulfadiazine

1. Introduction

Zeolites are crystalline microporous aluminosilicate materials possessing various functions.

There are approximately 250 zeolite frameworks with various porosities, pore sizes, and shapes, as well as interesting adsorption and ion-exchange properties that can be adjusted by controlling the $\text{SiO}_2/\text{Al}_2\text{O}_3$ ratio of the frameworks through the synthesis processes [1]. Owing to their diversity in microporous networks, zeolites have been extensively used in chemical industries as catalysts [2, 3], in agriculture and food production [4, 5], biotechnology and medicine [6], environmental detection [7, 8] and purification [9, 10]. Zeolites with high porosity and ion-exchange properties are effectively used to remove inorganic and organic pollutants in environmental applications [11].

Antibiotics are pharmaceutically active compounds used to treat infections in humans and livestock. It has been reported that antibiotic residues are detected in effluent from hospitals, livestock farms, and agriculture fields where manure fertilizers are used. Most antibiotics are not metabolized and thus persist in the environment. Therefore, they can enter water sources and harm aquatic organisms, leading to a high risk of environmental problems [12, 13]. Consequently, the removal of antibiotic residues from the water is necessary. Sulfonamide drugs, the sulfa drugs, cover a large group of

antibiotics; they have been widely used for a long time as veterinary drugs in animal feedstuffs and in human treatment to prevent infections such as the urinary tract infection [14, 15]. Sulfa drugs are water-soluble and are found in water worldwide [16]. Various treatment methods for the removal of antibiotics from various water bodies and systems have been reviewed [17, 18]. Among the reported methods, adsorption is a good choice because of its effectiveness and easy handling [18] as well as its broad applicability to both inorganic and organic pollutants [19].

High-silica zeolites with various zeolite frameworks, such as FAU [20-26], MOR [21, 27], MFI [21, 28], and low-silica zeolite (HEU) [29, 30] have been assessed for the removal of sulfonamide antibiotics from water. Each zeolite type reportedly shows potential for the adsorption of sulfonamide antibiotics. Another framework, the BEA-type, is a large-pore zeolite that has been characterized as a silica-rich structure with high hydrophobicity. Therefore, it is a promising adsorbent for removing organic pollutants along with other silica-rich zeolites [1].

Considering the separability of adsorbents from liquid media after adsorption, magnetic zeolite composites are more attractive choice than powdered non-magnetic zeolites because of their ease of recovery using an external magnetic field with a shorter collection time. Zeolites can be synthesized using the hydrothermal method, which is widely used for the preparation of magnetic zeolite composites [31-39]. Other wet and dry methods have been reported in the literature for preparing non-magnetic zeolites,

such as the alkaline molten-salt method [40], inter-zeolite conversion [41], mechanochemical synthesis [42], using hydrated alkaline silicate ionic liquids [43], solvent-free synthesis using organosilanes [44], and dry-gel conversion (DGC) [45-49]. Moreover, magnetic zeolite composite synthesis methods have been developed, with varieties such as the ionic exchange process [50], electrochemical synthesis in the presence of zeolites [51], chemical co-precipitation in the presence of zeolites [52], and maceration [53].

Regarding the synthesis of magnetic zeolite composites, controlling the crystallization of zeolites in the presence of magnetic particles to yield highly homogeneous magnetic composites remains challenging.

Our group has been paying special attention to the DGC method, first introduced to synthesize non-magnetic zeolite by Xu et al. in 1990 [45], owing to its high possibility of obtaining homogeneous magnetic zeolite composites. Additionally, the more rapid crystallization of zeolite compared to the common hydrothermal method can be restricted by the existence of a precursor using DGC. Since a dry-gel precursor is used, a lower reactor volume is required, and a high yield together with an extremely small amount of wastewater results in less waste production [46, 49]. In the dry-gel process, magnetic particles are initially mixed with ingredients of zeolites to form a uniform dry precursor gel before exposure to water vapor in the hydrothermal reactor. In this manner, the incorporation of magnetic particles with zeolite crystallization is accomplished. This method was successfully employed for the preparation of magnetic BEA-type zeolites, and their performance as adsorbents was tested for the

adsorption of an organic dye, which resulted in a high adsorption capacity [54]. However, the optimum dry-gel conversion synthesis conditions for magnetic BEA-type zeolites and their potential for antibiotic adsorption have not yet been clarified.

In this work, we synthesized magnetic BEA-type zeolites using the DGC method and investigated the optimal DGC synthesis conditions, namely the gel/water ratio, crystallization temperature, crystallization time, and calcination temperature. The magnetic BEA-type zeolite prepared under the optimum conditions was subsequently subjected to sulfadiazine adsorption as a model substance to represent sulfonamide antibiotics.

2. Materials and Methods

2.1 Materials

To synthesize magnetic BEA-type zeolites, colloidal silica (HS-30, 30 wt% silica, Sigma Aldrich, USA) as the silica source, aluminum sulfate hexahydrate ($\text{Al}_2(\text{SO}_4)_3 \cdot 16\text{H}_2\text{O}$, Nacalai Tesque, Kyoto, Japan) as the alumina source, sodium hydroxide (NaOH, Nacalai Tesque, Kyoto, Japan) as the alkali source, and tetraethylammonium hydroxide solution (TEAOH, 35 wt%, Tokyo Chemical Industry Co., Ltd., Tokyo, Japan) as the structure-directing agent (SDA) were used. Magnetite (Fe_3O_4 ; Kanto Chemical Co., Inc., Tokyo, Japan), having primary particle with Heywood diameters mostly in the range 100–300 nm (Fig. S1), was used as the magnetic material. Sulfadiazine ($\text{C}_{10}\text{H}_{10}\text{N}_4\text{O}_2\text{S}$, Tokyo Chemical

Industry Co., Ltd., Tokyo, Japan) was used as the model substance representing the sulfonamide antibiotic for evaluating the adsorption performance. 0.1 mol/L hydrochloric acid (HCl, Nacalai Tesque, Kyoto, Japan) solution, 0.1 mol/L NaOH solution were used to adjust initial pH and phosphate buffer pH 6.86 (Kanto Chemical Co., Inc., Tokyo, Japan) was used for measuring sulfadiazine concentrations in experiments considering pH effect on sulfadiazine adsorption.

2.2 Synthesis of magnetic BEA-type zeolites

The DGC synthesis conditions for magnetic BEA-type zeolites were considered using a fixed precursor gel prepared in the same manner as in our previous work [54]. Briefly, 12.10 g of colloidal silica, 9.42 g of 35wt% TEAOH solution, and 1.00 g of 20wt% NaOH solution were mixed and stirred for 30 min, with the subsequent addition of 10.64 g of 6wt% $\text{Al}_2(\text{SO}_4)_3 \cdot 16\text{H}_2\text{O}$ solution and 5.58 g of distilled water. The mixture was continuously stirred for 30 min before adding 1.12 g of Fe_3O_4 and stirred for another 30 min. The mixture was then heated to 80 °C to finally obtain dry-gel. The dry-gel was pulverized using a mortar before crystallization. A known weight of the precursor gel was placed in a PTFE cup and placed in a water-containing autoclave, operating at various gel/water ratios (0.5, 1, and 2). The DGC was then performed at various crystallization temperatures (140, 160, 180, and 200 °C) and crystallization times (1.5, 3, 6, and 12 h) in a water vapor-saturated atmosphere. The products were then dried without additional washing. X-ray diffraction (XRD, RINT 2500TTR, Rigaku Corporation, Japan)

with a Cu-K α radiation source ($\alpha = 1.54056 \text{ \AA}$) and scanning electron microscopy (SEM, JSM-6330F, JEOL, Japan) were used for characterization. The crystallized samples were further calcined in air at various temperatures (400, 450, and 500 °C) for 12 h to remove the SDA remaining in the zeolite pores. The magnetic properties of the calcined materials were evaluated by hysteresis loops measured using a vibrating-sample magnetometer (VSM, BH-5501, Denshijiki Industry Co. Ltd., Japan). The entire protocol was used but addition of Fe₃O₄ was excluded to synthesize non-magnetic BEA for comparison of morphology and adsorption performance.

2.3 Evaluation of sulfadiazine adsorption performance

The adsorption performance of the synthesized adsorbents was evaluated using adsorption isotherms. The isotherms were performed using 0.5 g/L adsorbent suspension in 10–50 mg/L sulfadiazine solutions as initial concentrations at pH 5.5 \pm 0.5. The suspensions were shaken for 24 h at 25 °C. The adsorbed amount and equilibrium concentration of sulfadiazine were calculated from the concentration of the sulfadiazine solutions before and after the adsorption test and were evaluated using a spectrophotometer ($\lambda = 264 \text{ nm}$, UV-2450, Shimadzu Co., Japan).

The effect of initial pH was also considered by adjusting the pH of 20 mg/L sulfadiazine solutions using 0.1 mol/L hydrochloric acid or 0.1 mol/L NaOH solution before adsorption. After 24 h adsorption at 25 °C, a constant volume of the supernatant was collected and diluted with phosphate buffer

pH 6.86 for evaluation of the adsorbed amount of sulfadiazine using a standard calibration curve prepared in phosphate buffer pH 6.86. Measurement of UV absorbance in the effect of initial pH test was performed at 240 nm.

2.4 Reusability of the adsorbents

To investigate the reusability of the adsorbents, 0.5 g/L of adsorbents were added in 20 mg/L sulfadiazine solution (pH 5.5±0.5) for 24 h. After adsorption for 24 h, the adsorbents were collected using a filter and were thermally regenerated at 400 °C for 12 h. The thermal treated adsorbents were used in subsequent numbers of adsorption/regeneration cycles. Equilibrium amount of sulfadiazine adsorbed (q_e , mg/g), was calculated to evaluate the reusability of the adsorbents.

3. Results and Discussions

3.1 Determination of optimal conditions for zeolite crystallization

The amount of water used as the steam source during the synthesis was determined by changing the gel/water ratios. It was found that the product was amorphous when a gel/water ratio of 2 was used, as no peaks of BEA-structure appeared in the XRD patterns (Fig. 1a), and no evidence of crystallization of BEA crystals could be seen from SEM images (Fig. 1b). The BEA-structure crystalline characteristic peaks, which agreed well with the standard card (JCPDS 48-0074), became highly intense when lower gel/water ratios of 1 and 0.5 were used. In addition, an obvious change in morphology was

observed at lower gel/water ratios of 1 and 0.5, supporting that crystallization of BEA zeolite took place.

The same results were obtained for both non-magnetic and magnetic zeolite samples. When using a gel/water ratio of 2, it was hypothesized that the amount of water was too low to sufficiently cause the reaction of the ingredients in the precursor gel to crystallize BEA. This finding supported a previous report that an amorphous product was obtained when the water amount was insufficient (higher gel/water ratios) [46]. Considering the lowest amount of water required among the studied conditions, a gel/water ratio of 1 was selected for further synthesis because it was sufficient to fully crystallize the BEA zeolite with and without the presence of Fe_3O_4 particles.

Numerous researchers have studied the effect of crystallization temperature during zeolite synthesis and proved that it has a significant influence on the crystallinity of zeolite products [33, 38, 49, 55-58]. In this work, we examined DGC temperature in the range 140–200 °C for 12 h at a constant reactant composition. As observed in the XRD patterns (Fig. 2a), crystalline BEA peaks were obtained, indicating crystalline BEA was formed at a crystallization temperature of 140 °C and became stronger up to 180 °C. However, much lower XRD peak intensity was found for that of magnetic BEA zeolite product at 140 °C compared to the non-magnetic one. It is assumed that the presence of Fe_3O_4 might have suppressed the nucleation and crystal growth rates at lower crystallization temperatures. This is also supported by the differences in the SEM images depicted in Fig. 2b, in which the formation of crystal-like

particles is not observed. At a higher crystallization temperature above 160 °C, crystalline rough spherical shape products were obviously obtained for both non-magnetic and magnetic BEA zeolites. Conversely, when the crystallization temperature increased to 200 °C, an amorphous phase was obtained in both non-magnetic and magnetic products, indicating the loss of crystallinity. This was possibly caused by the partial decomposition and evaporation of the SDA, as can be anticipated from the formation of small voids on the sample surface (see the higher magnification in Fig. 2b). By monitoring weight loss during calcination temperature study of zeolite BEA, do Nascimento et al. [59] found that decomposition of the organic TEOH template was observed from 200 °C, which supports the results of this work. Meanwhile, the characteristic peak of Fe₃O₄ at each studied temperature indicated that no phase change by oxidation occurred during the synthesis. The effect of the crystallization temperature was similar to that reported in previous studies, namely, that the phase change and decrease in the crystallinity of zeolites occurred at high crystallization temperatures [55, 57, 59, 60], and revealed that the formation of BEA-type zeolites strongly depends on the crystallization temperature. In this work, temperature in the range 160–180 °C was optimal for the crystallization of BEA with and without the presence of Fe₃O₄ particles. The adsorbent samples crystallized at 180 °C were used as the representatives for the study of crystallization time and evaluation of antibiotic adsorption performance.

Another influential parameter for both crystallinity and yield of the zeolite product is the

crystallization time. In this work, crystallization time in the range 1.5–12 h at a constant temperature (180 °C) and reactant composition were examined. It was found that crystalline BEA-type zeolite products could be formed even after a short crystallization time of 1.5 h, as shown in the XRD patterns (Fig. 3a). The peak intensity of BEA became more intense after longer crystallization times owing to the sufficient time for crystal growth. Well-formed spherical crystals of magnetic BEA were obtained after 3 h, as shown in Fig. 3b, but a constant yield was observed after 6 h and up to 12 h with the remaining Fe₃O₄ phase. Therefore, at least 6 h were required to reach saturated crystallization of BEA with and without the presence of Fe₃O₄ particles at 180 °C. To ensure that we obtained the optimal crystallinity and morphology, BEA and magnetic BEA samples crystallized at 180 °C, 12 h were selected for further evaluation of the effects of calcination temperature on their magnetic properties.

3.2 Investigation of magnetic properties of the calcined samples

Calcination is required to remove the organic template from the synthesized adsorbents and open their pores for adsorption. The magnetic properties of the magnetic BEA sample varied depending on the calcination temperature. As reported in the literature [59, 61], thermal gravimetric analysis of as-prepared BEA zeolite revealed that a dramatic decrease in the weight of the sample was found in the temperature range 400–500 °C, which is attributed to degradation of the organic SDA. Therefore, in this work, we examined the effect of this calcination temperature range on the magnetic properties of BEA

and magnetic BEA. Hysteresis loops of BEA and magnetic BEA-type zeolites crystallized at 180 °C (12 h) and calcined at 400, 450, and 500 °C (12 h), compared to bare Fe₃O₄, were measured using VSM at around 25 °C. The saturation magnetization (M_s) values, shown in Fig. 4a, of magnetic BEA samples that calcined at 400, 450, and 500 °C were 11.21, 7.58, and 2.52 emu/g, respectively. The saturation magnetization of the magnetic samples decreased with increasing calcination temperature. The synthesized magnetic BEA-type zeolites still exhibited ferromagnetic properties, although their M_s values were lower than that of bare Fe₃O₄ (73.949 emu/g), whereas the non-magnetic BEA samples did not show a magnetic response (Fig. 4b). A calcination temperature of approximately 500 °C was reported in the literature to effectively remove the organic template [59], but it also caused the magnetic properties to deteriorate due to oxidation of Fe₃O₄ to hematite (α -Fe₂O₃) phase, a soft magnetic material, at high temperatures [62]. The XRD pattern of the magnetic sample after calcination at 450 °C for 12 h showed the existence of α -Fe₂O₃ to some extent; however, the intensities of the characteristic peaks of Fe₃O₄ were only decreased in small quantity (data not shown). From the M_s data, magnetic contents in the samples calcined at 400 °C; where no oxidation of Fe₃O₄ was detected, was calculated to be 17.6 wt% but it decreased to 11.3 wt% after calcination at 450 °C. This loss of approximately one third of the apparent magnetic content after calcination at 450 °C could represent the amount of Fe₃O₄ oxidized to α -Fe₂O₃, which weakened the magnetic properties of the samples. Although, calcination at 450 °C partially

disturbed the magnetic properties, such temperature was necessary to degrade and remove the SDA from the adsorbent pores [59, 61] for sufficient adsorption of sulfadiazine. To compromise between magnetic separability and adsorption performance of the samples, the magnetic BEA calcined at 450 °C (12 h) was chosen for evaluation of sulfadiazine adsorption performance. The magnetic BEA calcined at 450 °C (12 h) still exhibited a good magnetic response and was quickly collected using a neodymium magnet (surface flux density of 0.45 T), unlike the non-magnetic ones with no attractivity.

3.3 Sulfadiazine adsorption performance test

Sulfadiazine adsorption isotherms of BEA and magnetic BEA zeolite samples calcined at 450 °C are shown in Fig. 5. The equilibrium sulfadiazine adsorption amount (q_e) increased with increasing sulfadiazine equilibrium concentrations. The adsorption amount of magnetic BEA seemed to be slightly lower than that of non-magnetic BEA. This was due to the incorporated amount of Fe_3O_4 , which did not contribute to the adsorption of sulfadiazine.

To explain the sulfadiazine adsorption behavior, two common adsorption models, the Langmuir and Freundlich models, were employed. The Langmuir model was constructed by plotting

C_e/q_e and C_e in the linear form:

$$\frac{C_e}{q_e} = \frac{C_e}{q_m} + \frac{1}{bq_m}$$

where C_e is the equilibrium concentration of sulfadiazine (mg/L), q_e is the equilibrium amount of sulfadiazine adsorbed (mg/g), q_m is the maximum adsorption capacity (mg/g), and b is the adsorption equilibrium constant (L/mg).

The Freundlich model was carried out by plotting $\log q_e$ and $\log C_e$ in the linear form of

$$\log q_e = \frac{1}{n} \log C_e + \log K_F$$

where K_F is a constant related to the relative adsorption capacity of the adsorbent ($\text{mg}^{1-(1/n)} \text{L}^{1/n} \text{g}^{-1}$) and n is a constant related to the intensity of the Freundlich adsorption. The linear plots in Fig. 6 indicate that the adsorption of sulfadiazine onto both BEA and magnetic BEA samples tended to fit the Freundlich isotherm, as indicated by the correlation coefficient (R^2). Therefore, the adsorption of sulfadiazine onto the BEA and magnetic BEA zeolites was multilayered, corresponding to physio sorption [63]. This finding was in good agreement with most of the previous studies; the adsorption isotherms of sulfadiazine [64, 65] and other sulfa drugs [22, 28, 30, 65-67] followed the Freundlich model, as summarized in Table 1. The values of n are greater than 1, indicating the favorable adsorption of neutral sulfadiazine onto both non-magnetic and magnetic BEA zeolites at the tested pH (5.5 ± 0.5). However, the Langmuir isotherm was also found to be a suitable model for sulfa drug adsorption onto high-silica zeolites in some literature [24, 66]. Considering the K_F values, which reflect the relative adsorption capacity, the magnetic BEA-

type zeolites could be a potential adsorbent for removing sulfonamide antibiotics from water in terms of adsorption performance and separability.

Sulfadiazine exists in neutral, and ionic forms depending on pH (Fig. 7). Therefore, the adsorption behavior of sulfadiazine on BEA zeolite and magnetic BEA zeolite composite could vary at different pH values. To explain the adsorption mechanism, adsorption of sulfadiazine was performed at pH 2.4, 4.4, 5.5±0.5, and 7.0 (using 20 mg/L sulfadiazine). After adsorption, pH of the solutions barely changed from the initial value (see Table S1). It was found that the UV absorption spectra of sulfadiazine changed according to pH (Fig. S2). Consequently, to measure the adsorbed amount of sulfadiazine, phosphate buffer (pH 6.86) was used to control the pH of the samples and the standard solutions. In this case, there were two strong absorption peaks at 240 and 257 nm which showed similar linearity (Fig. S3). The wavelength 240 nm was chosen as the analytical wavelength.

The pH of sulfadiazine solutions prepared without any adjustment was 5.5±0.5, where its neutral form is predominant (87.0%) and the rest 12.9% and 0.1% were the anionic and cationic form, respectively (Fig. 7). When the pH decreased from the original pH 5.5 to 4, the neutral form increased by 11.6% to become the most abundant form and the adsorbed amount also increased by similar percentage for non-magnetic BEA. This result indicated hydrophobic interaction between neutral sulfadiazine molecule and hydrophobic nature of the high-silica BEA was promoted at this pH. However, in case of

magnetic BEA, the increase in percentage of adsorbed amount was only half of the percentage increase in neutral form. This was due to the presence of iron oxide phase in the composite, which decreases the amount of the hydrophobic BEA and perhaps additionally due to the change in surface state of the adsorbent by the iron oxide phases. When the pH decreased from 4 to more acidic region, pH 2, the adsorbed amount of sulfadiazine greatly increased by more than 30% for both BEA and magnetic BEA, which was the highest level among the studied pH range. In this region, the fraction percentages of the cationic and neutral sulfadiazine were equal with negligible anionic form existed. Therefore, electrostatic interaction also may greatly contribute to the adsorption mechanism in addition to the hydrophobic interaction. The electrostatic interaction could be the ion-exchange between cationic sulfadiazine and the partially existing counter cation, Na^+ , at the alumina site of BEA. Moreover, according to the literature [68], surface charge of BEA (with $\text{SiO}_2/\text{Al}_2\text{O}_3$ ratio $\sim 15\text{--}30$) was negative over the pH range 2–11. This could be also preferable for attracting with the cationic sulfadiazine. Additionally, hydrogen bonds between nitrogen of sulfadiazine and the silanol group on BEA surface could also happen in acidic aqueous solution [69] or between amine hydrogen atom and oxygen atom in zeolite framework with medium strength [70]. Conversely, when the pH increased from the original 5.5 ± 0.5 to 7, the neutral form decreased about four times while the anionic form increased by six times becoming predominant (79.9%). The adsorbed amount of sulfadiazine dramatically decreased to nearly half for both BEA and magnetic

BEA, however; this decrease was milder than the percentage decrease in ionic state of sulfadiazine in neutral form (approximately -67%). The adsorbed amount was suppressed by the repulsion between the increased negative charged sulfadiazine and the alumina site of BEA. The non-proportional changes among fraction species and the suppressed adsorbed amount of sulfadiazine could be due to the remaining hydrophobic interaction which still mainly serves the adsorption process. The hydrophobic interaction was formed by attraction between aromatic rings on sulfadiazine and the siloxane network which is abundant in the high-silica zeolite framework [23]. Since the BEA and magnetic BEA were able to adsorb ionic and neutral sulfadiazine to some extent at the studied pH range. Thus, the hydrophobic interaction could occur mainly at wide pH range. This finding supports the previous research that the adsorption of sulfa drugs in neutral form *via* hydrophobic interaction is mainly preferable onto high-silica zeolite over the ionic forms [28, 65, 66].

3.4 Reusability and estimation for practical application

Regeneration of zeolites could vary depending on nature of the adsorbates which should be able to recover the adsorbents with maintained the structure and adsorption properties. Sulfadiazine is an organic substance that could be dissolved in an organic solvent or thermally decomposed. On the other hand, we found that the adsorption of sulfadiazine onto BEA zeolite was suppressed at higher pH. Therefore, in order to remove the adsorbed sulfadiazine from zeolites, some regeneration techniques such

as solvent extraction, thermal treatment, and washing by alkali solution seemed to be adoptable. Braschi et al. studied regeneration performance of sulfa drugs loaded high silica FAU zeolite. They found that the collected adsorbents that were washed using water/acetonitrile/methanol mixture and thermally treated at 500 °C showed the best regeneration performance [25]. In another paper, Sannino et al. regenerated sulfanilamide-adsorbed magnetic zeolites using thermal treatment at 400 °C, which found to fully recover the adsorbent properties. Additionally, they alternatively used diluted NaOH solution to wash the adsorbents which showed comparable performance [69]. In our studies, the stability of BEA structure and magnetic properties of magnetic BEA composite are both of concern. To ensure complete elimination of the adsorbed sulfadiazine we employed thermal treatment by re-calcination of the adsorbents at 400 °C for 12 h after each consecutive use. We investigated and compared the q_e values of three cycle-reused adsorbents and found that their q_e values after second and third adsorption cycles did not diminish, as shown in Fig. 8. Surprisingly, adsorption of sulfadiazine on BEA and magnetic BEA was slightly enhanced after regeneration. The explanation could be coming up with two possible reasons. First, Na^+ counter ions could have been replaced by the proton (H^+) presence in 20 mg/L sulfadiazine solution at pH 5.5, leaving behind more accessible area to sulfadiazine in the following adsorption/regeneration cycles. And second, re-calcination of the adsorbents at 400 °C for 12 h could release not only the adsorbed sulfadiazine but perhaps also the slightly remaining SDA (TEAOH) from the first calcination, which open

more pores ready to sulfadiazine in the following adsorption cycles. The magnetic properties of the magnetic BEA might not be suppressed after re-calcination since the XRD intensities of Fe_3O_4 and $\alpha\text{-Fe}_2\text{O}_3$ peaks remained unchanged (data not shown). Moreover, the reused magnetic BEA dispersed in aqueous solution still showed good attraction to the magnet. Therefore, the synthesized BEA and magnetic BEA could be reused for adsorption of sulfadiazine at least three cycles with improved performance.

The adsorption isotherm studies in this work using the initial sulfadiazine concentration in the range 10–50 mg/L reveal that the removal efficiency increased when the initial sulfadiazine concentrations decreased. Removal efficiency was ~48% at initial sulfadiazine concentration 10 mg/L and it became ~75% when the initial concentration of 1 mg/L was additionally tested using 1g/L of magnetic BEA sample. Typically, antibiotics in surface water and sewage treatment plant effluents or wastewaters are found in a rather lower range: 0.01–1.0 $\mu\text{g/L}$ [71], thus, the removal efficiency is expected to be higher than ~75%. From the aforementioned expectation, if 1000 L of wastewater, assumed to contain sulfadiazine concentration of 0.4 $\mu\text{g/L}$ at ~pH5.5, needs to be practically treated using an adsorbent with removal efficiency of ~75% and contact time of at least 1 h (reported time for sulfadiazine to reach saturation on zeolite [64]) shall reach the recommended discharge limit (0.1 $\mu\text{g/L}$), by US Food and Drug Administration [71] by using 1 kg of our magnetic adsorbents. The magnetic adsorbents could be

collected by using the water treatment system integrated with rotating magnetic separator [72]. After thermal regeneration, the magnetic adsorbents could be still reused for at least another 2 more cycles to reduce the assumed sulfadiazine amount in wastewater to below the discharge limit.

4. Conclusions

In this study, magnetic BEA-type zeolites were synthesized by dry-gel conversion method and the optimal synthesis conditions were determined. Magnetite, the selected as the magnetic particles, was well-mixed with the precursor dry gel before crystallization under a water vapor atmosphere. Optimal synthesis conditions, such as gel/water ratio, crystallization temperature, and crystallization time were investigated, and were found as 1, in the range 160–180 °C, and at least 6 h, respectively. Additionally, a calcination temperature of 450 °C is recommended to maintain both adsorption and magnetic properties of the magnetic BEA-type zeolites. In this manner, uniform magnetic BEA-type zeolites with good magnetic separability were obtained. The performance of the synthesized non-magnetic and magnetic adsorbents was evaluated by the adsorption of sulfadiazine, a sulfonamide antibiotic, in aqueous solutions. The adsorption was found to be of a multilayer type and followed to the Freundlich model. The dry-gel conversion method is therefore well-suited for the preparation of high-silica magnetic zeolites with potential for antibiotic removal.

Acknowledgment

This work was partially supported by the Strategic International Collaborative Research Program (SICORP) [grant number JPMJSC18H1] from the Japan Science and Technology Agency, a research grant from Kyosho Hatta foundation, Japan and the National Key Research and Development Program of China [grant number 2017YFE0127100]. In addition, we express our gratitude to Kiwamu Oda, Nagoya Municipal Industrial Research Institute, for assistance in measurements of magnetic properties and also to Editage for English language editing.

Competing Interests

The authors have no relevant financial or non-financial interests to disclose.

Author Contributions

Conceptualization: Takeshi Hagio; Data curation: Vanpaseuth Phouthavong; Formal analysis: Vanpaseuth Phouthavong, Masatake Hiraiwa, Jae-Hyeok Park; Funding acquisition: Ryoichi Ichino; Investigation: Vanpaseuth Phouthavong, Takeshi Hagio, Masatake Hiraiwa; Methodology: Takeshi Hagio; Project administration: Takeshi Hagio; Resources: Ratana Rujiravanit, Yuki Kamimoto; Supervision: Takeshi Hagio, Ryoichi Ichino, Ratana Rujiravanit, Liang Li; Validation: Teeranun Srihirunthanon, Nutchanan Chantanurak, Supinya Nijpanich; Visualization: Vanpaseuth Phouthavong, Long Kong; Writing – original draft preparation: Vanpaseuth Phouthavong, Takeshi Hagio; Writing – review and editing: Jae-Hyeok Park, Supinya Nijpanich, Xinling Li, Long Kong, Liang Li. All authors read and approved the

final manuscript.

References

- [1] Jiang N, Shang R, Heijman SGJ, Rietveld LC (2018) High-silica zeolites for adsorption of organic micro-pollutants in water treatment: A review. *Water Res* 144:145–161. <https://doi.org/10.1016/j.watres.2018.07.017>
- [2] Naber JE, de Jong KP, Stork WHJ, Kuipers HPCE, Post MFM (1994) Industrial applications of zeolite catalysis. *Stud Surf Sci Catal* 84:2197–2219. [https://doi.org/10.1016/S0167-2991\(08\)63783-0](https://doi.org/10.1016/S0167-2991(08)63783-0)
- [3] Yilmaz B, Müller U (2009) Catalytic applications of zeolites in chemical industry. *Top Catal* 52:888–895. <https://doi.org/10.1007/s11244-009-9226-0>
- [4] Eroglu N, Emekci M, Athanassiou CG (2017) Applications of natural zeolites on agriculture and food production. *J Sci Food Agric* 97:3487–3499. <https://doi.org/10.1002/jsfa.8312>
- [5] Ramesh K, Reddy DD (2011) Zeolites and their potential uses in agriculture. In Sparks DL (ed) *Advances in Agronomy*, Academic Press, New York, pp 219–241
- [6] Bacakova L, Vandrovцова M, Kopova I, Jirka I (2018) Applications of zeolites in biotechnology and medicine – A review. *Biomater Sci* 6:974–989. <https://doi.org/10.1039/C8BM00028J>
- [7] Valdés MG, Pérez-Cordoves AI, Díaz-García ME (2006) Zeolites and zeolite-based materials in analytical chemistry. *TrAC Trends Anal Chem* 25:24–30. <https://doi.org/10.1016/j.trac.2005.04.016>
- [8] Jalili V, Barkhordari A, Ghiasvand A (2020) New extraction media in microextraction techniques. A review of reviews. *Microchem J* 153:104368. <https://doi.org/10.1016/j.microc.2019.104386>
- [9] Misaelides P (2011) Application of natural zeolites in environmental remediation: A short review. *Micropor Mesopor Mater* 144:15–18. <https://doi.org/10.1016/j.micromeso.2011.03.024>

- [10] Montalvo S, Huiliñir C, Borja R, Sánchez E, Herrmann C (2020) Application of zeolites for biological treatment processes of solid wastes and wastewaters – A review. *Bioresour Technol* 301:122808. <https://doi.org/10.1016/j.biortech.2020.122808>
- [11] Khaleque A, Alam MdM, Hoque M, Mondal S, Haider JB, Xu B, Johir MAH, Karmakar AK, Zhou JL, Ahmed MB, Moni MA (2020) Zeolite synthesis from low-cost materials and environmental applications: A review. *Environmental Advances* 2:100019. <https://doi.org/10.1016/j.envadv.2020.100019>
- [12] Seifrtová M, Nováková L, Lino C, Pena A, Solich P (2009) An overview of analytical methodologies for the determination of antibiotics in environmental waters. *Anal Chim Acta* 649:158–179. <https://doi.org/10.1016/j.aca.2009.07.031>
- [13] Polianciuc SI, Gurzău AE, Kiss B, Ștefan MG, Loghin F (2020) Antibiotics in the environment: Causes and consequences. *Med Pharm Rep* 93:231–240. <https://doi.org/10.15386/mpr-1742>
- [14] Dadfarnia S, Hajishabani AM, Rad HF (2011) Indirect determination of sulfadiazine by cloud point extraction/flow injection-flame atomic absorption (CPE/FI-FAAS) spectrometry. *J Chin Chem Soc* 58:503–508. <https://doi.org/10.1002/JCCS.201190013>
- [15] Liu K, Xu S, Zhang M, Kou Y, Zhou X, Luo K, Hu L, Liu X, Liu M, Bai L (2016) Estimation of the toxicity of sulfadiazine to *Daphnia magna* using negligible depletion hollow-fiber liquid-phase microextraction independent of ambient pH. *Sci Rep* 6:39798. <https://doi.org/10.1038/srep39798>
- [16] Paumelle M, Donnadiou F, Joly M, Besse-Hoggan P, Artigas J (2021) Effects of sulfonamide antibiotics on aquatic microbial community composition and functions. *Environ Int* 146:106198. <https://doi.org/10.1016/j.envint.2020.106198>
- [17] Phoon BL, Ong CC, Mohamed Saheed MSM, Show PL, Chang JS, Ling TC, Lam SS, Juan JC (2020) Conventional and emerging technologies for removal of antibiotics from wastewater. *J Hazard Mater* 400:122961. <https://doi.org/10.1016/j.jhazmat.2020.122961>

- [18] Lu ZY, Ma YL, Zhang JT, Fan NS, Huang BC, Jin RC (2020) A critical review of antibiotic removal strategies: Performance and mechanisms. *J Water Process Eng* 38:101681. <https://doi.org/10.1016/j.jwpe.2020.101681>
- [19] Gupta VK, Carrott PJM, Ribeiro Carrott MML, Suhas (2009) Low-cost adsorbents: Growing approach to wastewater treatment – A review. *Crit Rev Environ Sci Technol* 39:783–842. <https://doi.org/10.1080/10643380801977610>
- [20] Braschi I, Blasioli S, Gigli L, Gessa CE, Alberti A, Martucci A (2010) Removal of sulfonamide antibiotics from water: Evidence of adsorption into an organophilic zeolite Y by its structural modifications. *J Hazard Mater* 178:218–225. <https://doi.org/10.1016/j.jhazmat.2010.01.066>
- [21] Blasioli S, Martucci A, Paul G, Gigli L, Cossi M, Johnston CT, Marchese L, Braschi I (2014) Removal of sulfamethoxazole sulfonamide antibiotic from water by high silica zeolites: A study of the involved host–guest interactions by a combined structural, spectroscopic, and computational approach. *J Colloid Interface Sci* 419:148–159. <https://doi.org/10.1016/j.jcis.2013.12.039>
- [22] de Sousa DNR, Insa S, Mozeto AA, Petrovic M, Chaves TF, Fadini PS (2018) Equilibrium and kinetic studies of the adsorption of antibiotics from aqueous solutions onto powdered zeolites. *Chemosphere* 205:137–146. <https://doi.org/10.1016/j.chemosphere.2018.04.085>
- [23] Fukahori S, Fujiwara T, Funamizu N, Matsukawa K, Ito R (2013) Adsorptive removal of sulfonamide antibiotics in livestock urine using the high-silica zeolite HSZ-385. *Water Sci Technol* 67:319–325. <https://doi.org/10.2166/wst.2012.513>
- [24] Fukahori S, Fujiwara T (2014) Modeling of sulfonamide antibiotic removal by TiO₂/high-silica zeolite HSZ-385 composite. *J Hazard Mater* 272:1–9. <https://doi.org/10.1016/j.jhazmat.2014.02.028>
- [25] Braschi I, Blasioli S, Buscaroli E, Montecchio D, Martucci A (2016) Physicochemical regeneration of high silica zeolite Y used to clean-up water polluted with sulfonamide antibiotics.

- J Environ Sci 43:302–312. <https://doi.org/10.1016/j.jes.2015.07.017>
- [26] Braschi I, Martucci A, Blasioli S, Mzini LL, Ciavatta C, Cossi M (2016) Effect of humic monomers on the adsorption of sulfamethoxazole sulfonamide antibiotic into a high silica zeolite Y: An interdisciplinary study. *Chemosphere* 155:444–452. <https://doi.org/10.1016/j.chemosphere.2016.04.008>
- [27] Martucci A, Cremonini MA, Blasioli S, Gigli L, Gatti G, Marchese L, Braschi I (2013) Adsorption and reaction of sulfachloropyridazine sulfonamide antibiotic on a high silica mordenite: A structural and spectroscopic combined study. *Micropor Mesopor Mater* 170:274–286. <https://doi.org/10.1016/j.micromeso.2012.11.031>
- [28] Zuo X, Qian C, Ma S, Xiong J (2020) Sulfonamide antibiotics sorption by high silica ZSM-5: Effect of pH and humic monomers (vanillin and caffeic acid). *Chemosphere* 248:126061. <https://doi.org/10.1016/j.chemosphere.2020.126061>
- [29] Li Z, Stockwell C, Niles J, Minegar S, Hong H (2013) Uptake of sulfadiazine sulfonamide from water by clinoptilolite. *Appl Environ Soil Sci* 2013:1–8. <https://doi.org/10.1155/2013/648697>
- [30] Liu Y, Liu X, Lu S, Zhao B, Wang Z, Xi B, Guo W (2020) Adsorption and biodegradation of sulfamethoxazole and ofloxacin on zeolite: Influence of particle diameter and redox potential. *Chem Eng J* 384:123346. <https://doi.org/10.1016/j.cej.2019.123346>
- [31] Peng ZD, Lin XM, Zhang YL, Hu Z, Yang XJ, Chen CY, Chen HY, Li YT, Wang JJ (2021) Removal of cadmium from wastewater by magnetic zeolite synthesized from natural, low-grade molybdenum. *Sci Total Environ* 772:145355. <https://doi.org/10.1016/j.scitotenv.2021.145355>
- [32] Cheng Y, Xu L, Jiang Z, Liu C, Zhang Q, Zou Y, Chen Y, Li J, Liu X (2021) Feasible low-cost conversion of red mud into magnetically separated and recycled hybrid SrFe₁₂O₁₉@NaP1 zeolite as a novel wastewater adsorbent. *Chem Eng J* 417:128090. <https://doi.org/10.1016/j.cej.2020.128090>
- [33] Ye C, Lu P, Jiang X, Wu C, Qiu T, Li Y (2020) Synthesis and adsorption behavior of a magnetic

- ZSM zeolite for the selective removal of p-xylene from complex aqueous media. *Chem Eng Process* 153:107961. <https://doi.org/10.1016/j.cep.2020.107961>
- [34] Hagio T, Kunishi H, Yamaoka K, Kamimoto Y, Ichino R (2018) Seed-assisted synthesis of magnetic faujasite-type zeolite and its adsorption performance. *Nanosci Nanotechnol Lett* 10:862–867. <https://doi.org/10.1166/nml.2018.2640>
- [35] Aono H, Kaji N, Itagaki Y, Johan E, Matsue N (2016) Synthesis of mordenite and its composite material using chemical reagents for Cs decontamination. *J Ceram Soc Jpn* 124:617–623. <https://doi.org/10.2109/jcersj2.15317>
- [36] Cao J, Chang G, Guo H, Chen J (2013) Synthesis and characterization of magnetic ZSM-5 zeolite. *Trans Tianjin Univ* 19:326–331. <https://doi.org/10.1007/s12209-013-1912-0>
- [37] Liu H, Peng S, Shu L, Chen T, Bao T, Frost RL (2013) Effect of Fe₃O₄ addition on removal of ammonium by zeolite NaA. *J Colloid Interface Sci* 390:204–210. <https://doi.org/10.1016/j.jcis.2012.09.010>
- [38] Liu H, Peng S, Shu L, Chen T, Bao T, Frost RL (2013) Magnetic zeolite NaA: Synthesis, characterization based on metakaolin and its application for the removal of Cu²⁺, Pb²⁺. *Chemosphere* 91:1539–1546. <https://doi.org/10.1016/j.chemosphere.2012.12.038>
- [39] Cao JL, Liu XW, Fu R, Tan ZY (2008) Magnetic P zeolites: Synthesis, characterization and the behavior in potassium extraction from seawater. *Sep Purif Technol* 63:92–100. <https://doi.org/10.1016/j.seppur.2008.04.015>
- [40] Park M, Choi CL, Lim WT, Kim MC, Choi J, Heo NH (2000) Molten-salt method for the synthesis of zeolitic materials I. *Micropor Mesopor Mater* 37:81–89. [https://doi.org/10.1016/S1387-1811\(99\)00196-1](https://doi.org/10.1016/S1387-1811(99)00196-1)
- [41] Inoue T, Itakura M, Jon H, Oumi Y, Takahashi A, Fujitani T, Sano T (2009) Synthesis of LEV zeolite by interzeolite conversion method and its catalytic performance in ethanol to olefins reaction. *Micropor Mesopor Mater* 122:149–154.

- <https://doi.org/10.1016/j.micromeso.2009.02.027>
- [42] Ren L, Wu Q, Yang C, Zhu L, Li C, Zhang P, Zhang H, Meng X, Xiao FS (2012) Solvent-free synthesis of zeolites from solid raw materials. *J Am Chem Soc* 134:15173–15176. <https://doi.org/10.1021/ja3044954>
- [43] van Tendeloo L, Haouas M, Martens JA, Kirschhock CEA, Breynaert E, Taulelle F (2015) Zeolite synthesis in hydrated silicate ionic liquids. *Faraday Discuss* 179:437–449. <https://doi.org/10.1039/c4fd00234b>
- [44] Petkowicz DI, Canal S, Finger PH, Mignoni ML, dos Santos JHZ (2017) Synthesis of hybrid zeolites using a solvent-free method in the presence of different organosilanes. *Micropor Mesopor Mater* 241:98–106. <https://doi.org/10.1016/j.micromeso.2016.11.030>
- [45] Xu W, Dong J, Li J, Li J, Wu F (1990) A novel method for the preparation of zeolite ZSM-5. *J Chem Soc Chem Commun* 10:755–756. <https://doi.org/10.1039/C39900000755>
- [46] Rao PRHP, Matsukata M (1996) Dry-gel conversion technique for synthesis of zeolite BEA. *Chem Commun* 12:1441–1442. <https://doi.org/10.1039/CC9960001441>
- [47] Weitkamp J, Hunger M (2005) Preparation of zeolites via the dry-gel synthesis method. *Stud Surf Sci Catal* 155:1–12. [https://doi.org/10.1016/S0167-2991\(05\)80133-8](https://doi.org/10.1016/S0167-2991(05)80133-8)
- [48] Goergen S, Saada MA, Soulard M, Rouleau L, Patarin J (2010) Dry gel conversion synthesis of shape controlled MFI type zeolite materials. *J Porous Mater* 17:635–641. <https://doi.org/10.1007/S10934-009-9333-0>
- [49] Mohammadparast F, Halladj R, Askari S (2018) The synthesis of nano-sized ZSM-5 zeolite by dry gel conversion method and investigating the effects of experimental parameters by Taguchi experimental design. *J Exp Nanosci* 13:160–173. <https://doi.org/10.1080/17458080.2018.1453172>
- [50] Falyouna O, Eljamal O, Maamoun I, Tahara A, Sugihara Y (2020) Magnetic zeolite synthesis for efficient removal of cesium in a lab-scale continuous treatment system. *J Colloid Interface Sci*

- 571:66–79. <https://doi.org/10.1016/j.jcis.2020.03.028>
- [51] Piri F, Mollahosseini A, Khadir A, Milani Hosseini MM (2019) Enhanced adsorption of dyes on microwave-assisted synthesized magnetic zeolite–hydroxyapatite nanocomposite. *J Environ Chem Eng* 7:103338. <https://doi.org/10.1016/j.jece.2019.103338>
- [52] Gaffer A, Al Kahlawy AAA, Aman D (2017) Magnetic zeolite-natural polymer composite for adsorption of chromium (VI). *Egypt J Pet* 26:995–999. <https://doi.org/10.1016/j.ejpe.2016.12.001>
- [53] Bessa RdA, Costa LdS, Oliveira CP, Bohn F, do Nascimento RF, Sasaki JM, Loiola AR (2017) Kaolin-based magnetic zeolites A and P as water softeners. *Micropor Mesopor Mater* 245:64–72. <https://doi.org/10.1016/j.micromeso.2017.03.004>
- [54] Phouthavong V, Hiraiwa M, Hagio T, Nijpanich S, Chounlamany V, Nishihama T, Kamimoto Y, Ichino R (2020) Magnetic BEA-type zeolites: Preparation by dry-gel conversion method and assessment of dye removal performance. *J Mater Cycles Waste Manag* 22:375–382. <https://doi.org/10.1007/s10163-020-00994-8>
- [55] Alipour SM, Halladj R, Askari S (2014) Effects of the different synthetic parameters on the crystallinity and crystal size of nanosized ZSM-5 zeolite. *Rev Chem Eng* 30:289–322. <https://doi.org/10.1515/revce-2014-0008>
- [56] Chen YH, Han DM, Cui HX, Zhang Q (2019) Synthesis of ZSM-5 via organotemplate-free and dry gel conversion method: Investigating the effects of experimental parameters. *J Solid State Chem* 279:120969. <https://doi.org/10.1016/j.jssc.2019.120969>
- [57] Karimi R, Bayati B, Charchi Aghdam NC, Ejtemaee M, Babaluo AA (2012) Studies of the effect of synthesis parameters on ZSM-5 nanocrystalline material during template-hydrothermal synthesis in the presence of chelating agent. *Powder Technol* 229:229–236. <https://doi.org/10.1016/j.powtec.2012.06.037>
- [58] Modhera B, Chakraborty M, Parikh PA, Jasra RV (2009) Synthesis of nano-crystalline zeolite β :

- Effects of crystallization parameters. *Cryst Res Technol* 44:379–385.
<https://doi.org/10.1002/crat.200800474>
- [59] R. do Nascimento A, P. de Figueredo G, F. Silva EM, de F. Melo MA, de A. Melo DM, B. de Souza MJ (2017) Synthesis, optimization and characterization of zeolite beta (BEA): Production of ZSM-5 and NaAlSiO₄ as secondary phases. *Rev Virtual Quím* 9:1570–1582.
<https://doi.org/10.21577/1984-6835.20170092>
- [60] Nakai M, Miyake K, Inoue R, Ono K, Al Jabri HA, Hirota Y, Uchida Y, Miyamoto M, Nishiyama N (2019) Synthesis of high silica *BEA type ferrisilicate (Fe-Beta) by dry gel conversion method using dealuminated zeolites and its catalytic performance on acetone to olefins (ATO) reaction. *Micropor Mesopor Mater* 273:189–195.
<https://doi.org/10.1016/j.micromeso.2018.06.008>
- [61] Huang Z, Su JF, Guo YH, Su XQ, Teng LJ (2009) Synthesis of well-crystallized zeolite beta at large scale and its incorporation into polysulfone matrix for gas separation. *Chem Eng Commun* 196:969–986. <https://doi.org/10.1080/00986440902797824>
- [62] Li YS, Church JS, Woodhead AL (2012) Infrared and Raman spectroscopic studies on iron oxide magnetic nano-particles and their surface modifications. *J Magn Magn Mater* 324:1543–1550. <https://doi.org/10.1016/j.jmmm.2011.11.065>
- [63] Alnajrani MN, Alsager OA (2020) Removal of antibiotics from water by polymer of intrinsic microporosity: Isotherms, kinetics, thermodynamics, and adsorption mechanism. *Sci Rep* 10:794.
<https://doi.org/10.1038/s41598-020-57616-4>
- [64] Liu X, Liu Y, Lu S, Guo W, Xi B (2018) Performance and mechanism into TiO₂/zeolite composites for sulfadiazine adsorption and photodegradation. *Chem Eng J* 350:131–147.
<https://doi.org/10.1016/j.cej.2018.05.141>
- [65] Zuo X, Qian C, Ma S, Xiong J, He J, Chen Z (2019) Removal of sulfonamide antibiotics from water by high-silica ZSM-5. *Water Sci Technol* 80:507–516.

- <https://doi.org/10.2166/wst.2019.294>
- [66] Fukahori S, Fujiwara T, Ito R, Funamizu N (2011) pH-dependent adsorption of sulfa drugs on high silica zeolite: Modeling and kinetic study. *Desalination* 275:237–242. <https://doi.org/10.1016/j.desal.2011.03.006>
- [67] Doekhi-Bennani Y, Leilabady NM, Fu M, Rietveld LC, van der Hoek JP, Heijman SGJ (2021) Simultaneous removal of ammonium ions and sulfamethoxazole by ozone regenerated high silica zeolites. *Water Res* 188:116472. <https://doi.org/10.1016/j.watres.2020.116472>
- [68] Yang W, Wang X, Tang Y, Wang Y, Ke C, Fu C (2002) Layer-by-layer assembly of nanozeolite based on polymeric microsphere: Zeolite coated sphere and hollow zeolite sphere. *J Macromol Sci Pure Appl Chem* 39:509–526. <http://doi.org/10.1081/MA-120004244>
- [69] Sannino F, Pansini M, Marocco A, Cinquegrana A, Esposito S, Tammaro O, Barrera G, Tiberto P, Allia P, Pirozzi D (2022) Removal of sulfanilamide by tailor-made magnetic metal-ceramic nanocomposite adsorbents. *J Environ Manag* 310:114701. <http://doi.org/10.1016/j.jenvman.2022.114701>
- [70] Braschi I, Gatti G, Paul G, Gessa CE, Cossi M, Marchese L (2010) Sulfonamide antibiotics embedded in high silica zeolite Y: A combined experimental and theoretical study of host-guest and guest-guest interactions. *Langmuir* 26:9524–9532. <http://doi.org/10.1021/la904913z>
- [71] Le Page G, Gunnarasson L, Snape J, Tyler CR, Cossi M (2017) Integrating human and environmental health in antibiotic risk assessment: A critical analysis of protection goals, species sensitivity and antimicrobial resistance. *Environ Int* 109:155–169. <http://doi.org/10.1016/j.envint.2017.09.013>
- [72] Hitachi (2022) Flocculation and magnetic separation system. https://www.hitachi.com/businesses/infrastructure/product_site/water_environment/fms/index.html. Accessed 4 Nov 2022

Figure captions

Fig. 1 a) XRD patterns and **b)** SEM images of BEA and magnetic BEA-type zeolites synthesized using different gel/water ratios, at 180 °C for 12 h

Fig. 2 a) XRD patterns and **b)** SEM images of BEA and magnetic BEA-type zeolites synthesized using gel/water ratio of 1 at different crystallization temperatures for 12 h

Fig. 3 a) XRD patterns and **b)** SEM images of BEA and magnetic BEA-type zeolites synthesized using gel/water ratio of 1 at 180 °C for different crystallization times

Fig. 4 Magnetization curves of **a)** magnetic BEA, denoted as MBEA, and **b)** BEA measured at room temperature in comparison with Fe₃O₄. Numbers in the data series names represent calcination temperatures in °C

Fig. 5 Adsorption isotherm of sulfadiazine onto BEA and magnetic BEA-type zeolites calcined at 450 °C

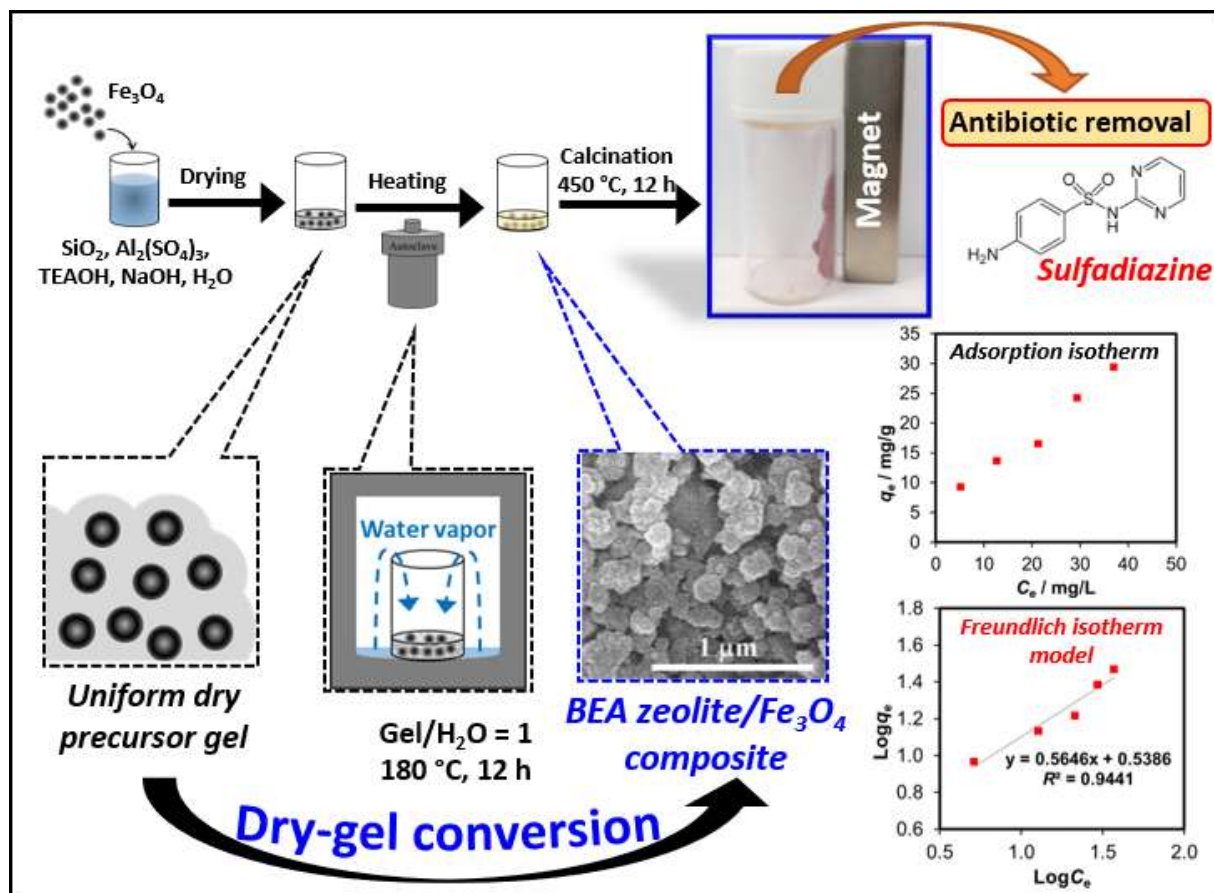
Fig. 6 Adsorption isotherm plots using Langmuir and Freundlich models of sulfadiazine onto BEA and magnetic BEA-type zeolites calcined at 450 °C

Fig. 7 Fraction species and adsorbed amount percentage of sulfadiazine on BEA (circle marker) and magnetic BEA (diamond marker) at different pH values. The adsorbed amount percentage was calculated as per total amount of sulfadiazine in the initial solutions (20 mg/L)

Fig. 8 Equilibrium amount of sulfadiazine adsorbed on BEA and magnetic BEA after each

adsorption/regeneration cycle

Graphical abstract



Graphical abstract shows the synthesis of BEA zeolite/Fe₃O₄ composite via dry-gel conversion method; a novel composite synthesis method first proposed by our group, and its potential to apply for antibiotics removal. The experimental scheme represents the unique synthesis process of the composite by mixing raw materials for zeolite with the Fe₃O₄ particles before drying to obtain uniform dry zeolite precursor gel containing Fe₃O₄ followed by crystallization. Highly crystalline BEA zeolite could be crystallized under saturated water vapor by heating the dry gel in a closed autoclave containing small amount of water under modified conditions. The effects of gel/H₂O ratio, crystallization temperature, and crystallization time on crystallization of the composite adsorbent were studied and the optimized condition was found to be gel/H₂O = 1, crystallization temperature of 180 °C, and crystallization time of 12 h. The SEM image

reveals that the composite adsorbent obtained under the aforementioned optimized condition results in uniform crystals with small size below 1 μm and isotropic shape. The top right picture proves that calcined BEA zeolite/ Fe_3O_4 composite allows simple magnetic separation using a magnet which was further tested for removal of antibiotics (sulfadiazine) from water. The experimental adsorption isotherm plot shows that the BEA zeolite/ Fe_3O_4 composite can remove sulfadiazine through adsorption, and the adsorption was found to well fit to linear Freundlich isotherm model.

Table 1 Freundlich isotherm parameters for sulfa drug adsorption onto BEA, magnetic BEA-type zeolites

in this work, and in previous reported zeolites

Zeolite (SiO ₂ /Al ₂ O ₃ ratio)	Sulfa drugs	Freundlich adsorption isotherm parameters			References
		K_F (mg ^{1-(1/n)} L ^{1/n} g ⁻¹)	n	R^2	
FAU (100)	Sulfamethoxazole	8611.5 ^a	2.92	0.971	[66]
FAU (30.62)	Sulfamethoxazole	26.10	0.64	0.998	[22]
FAU (82.59)	Sulfamethoxazole	105.46	0.54	0.994	[22]
HEU (\approx 12.5) ^d	Sulfamethoxazole	2.65	2.23	0.978	[30]
MFI (500)	Sulfamethoxazole	20.97	1.74	0.96	[28]
MFI (500)	Sulfamethoxazole	42.66	1.393	0.952	[65]
MOR (\approx 40) ^e	Sulfamethoxazole ^c	9.63 ^b	1.00	0.991	[67]
TiO ₂ /HEU (Not reported)	Sulfadiazine	0.0811	0.9077	0.9593	[64]
MFI (500)	Sulfadiazine	5.68	1.21	0.99	[28]
MFI (500)	Sulfadiazine	2.74	2.134	0.970	[65]
BEA (44)	Sulfadiazine	3.424	1.531	0.9967	This study
Magnetic BEA (44)	Sulfadiazine	3.456	1.771	0.9441	This study

a: recalculated from the original value of 0.034 mol^{1-(1/n)} L^{1/n} g⁻¹ [66]; b: the original unit is $\mu\text{g/g}$ (L/ μg)ⁿ [67]; c:

tested with co-existing of ammonium ion [67]; d: calculated using the reported weight percentage of SiO₂ (68.60

wt%) and Al₂O₃ (9.33 wt%) in the commercial zeolite [30]; e: recalculated from the reported weight percentage of

SiO₂ (94.656 wt%) and Al₂O₃ (3.933 wt%) [67].

Fig. 1 a) XRD patterns and b) SEM images of BEA and magnetic BEA-type zeolites synthesized using different gel/water ratios, at 180 °C for 12 h

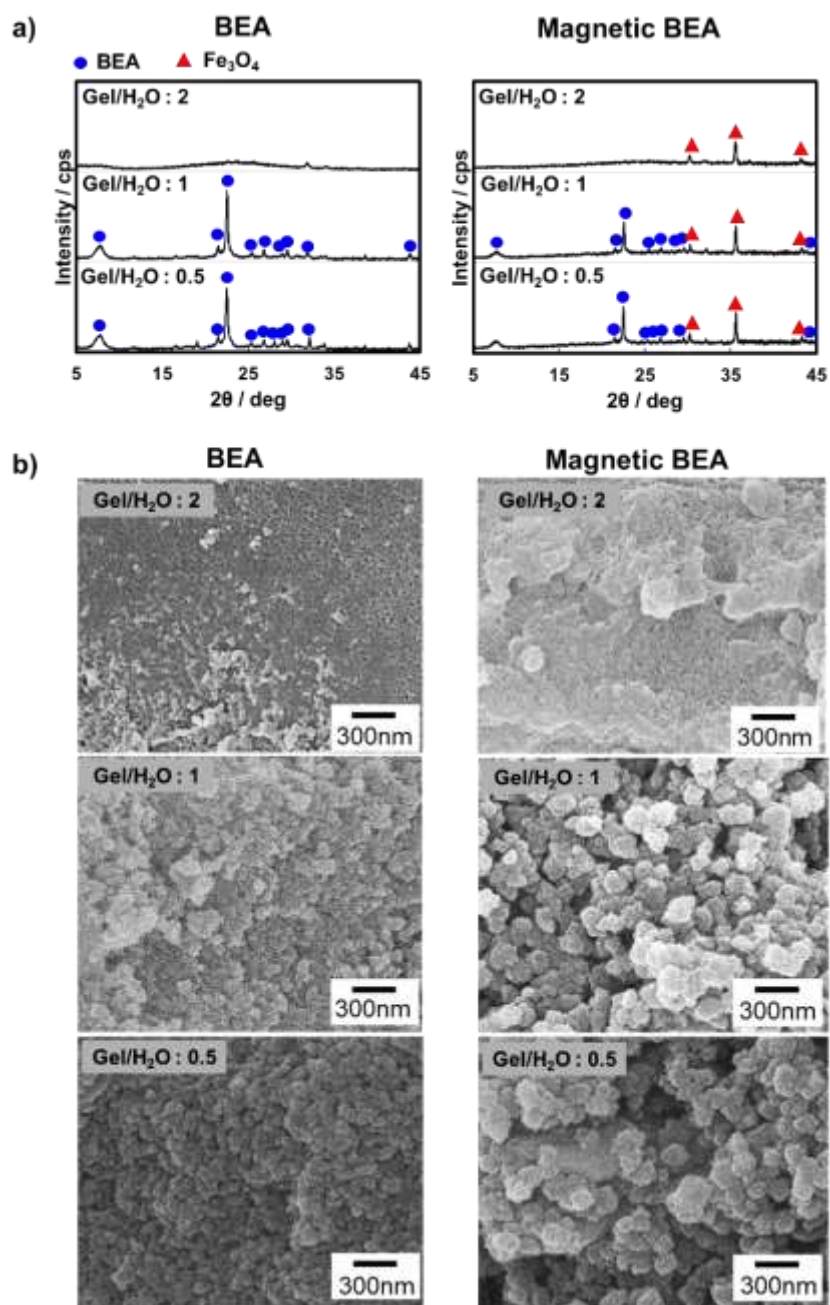


Fig. 2 a) XRD patterns and **b)** SEM images of BEA and magnetic BEA-type zeolites synthesized using

gel/water ratio of 1 at different crystallization temperatures for 12 h

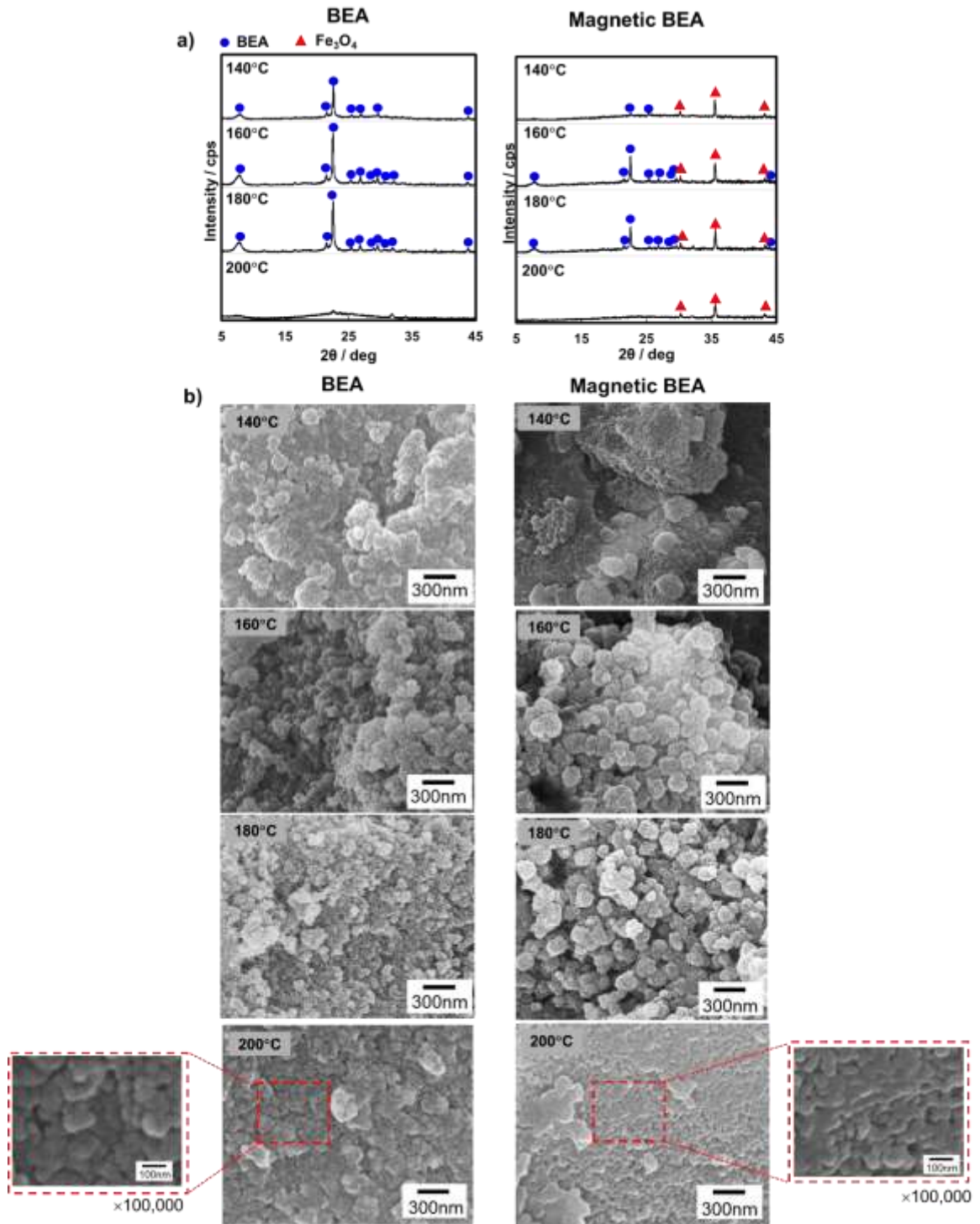


Fig. 3 a) XRD patterns and b) SEM images of BEA and magnetic BEA-type zeolites synthesized using gel/water ratio of 1 at 180 °C for different crystallization times

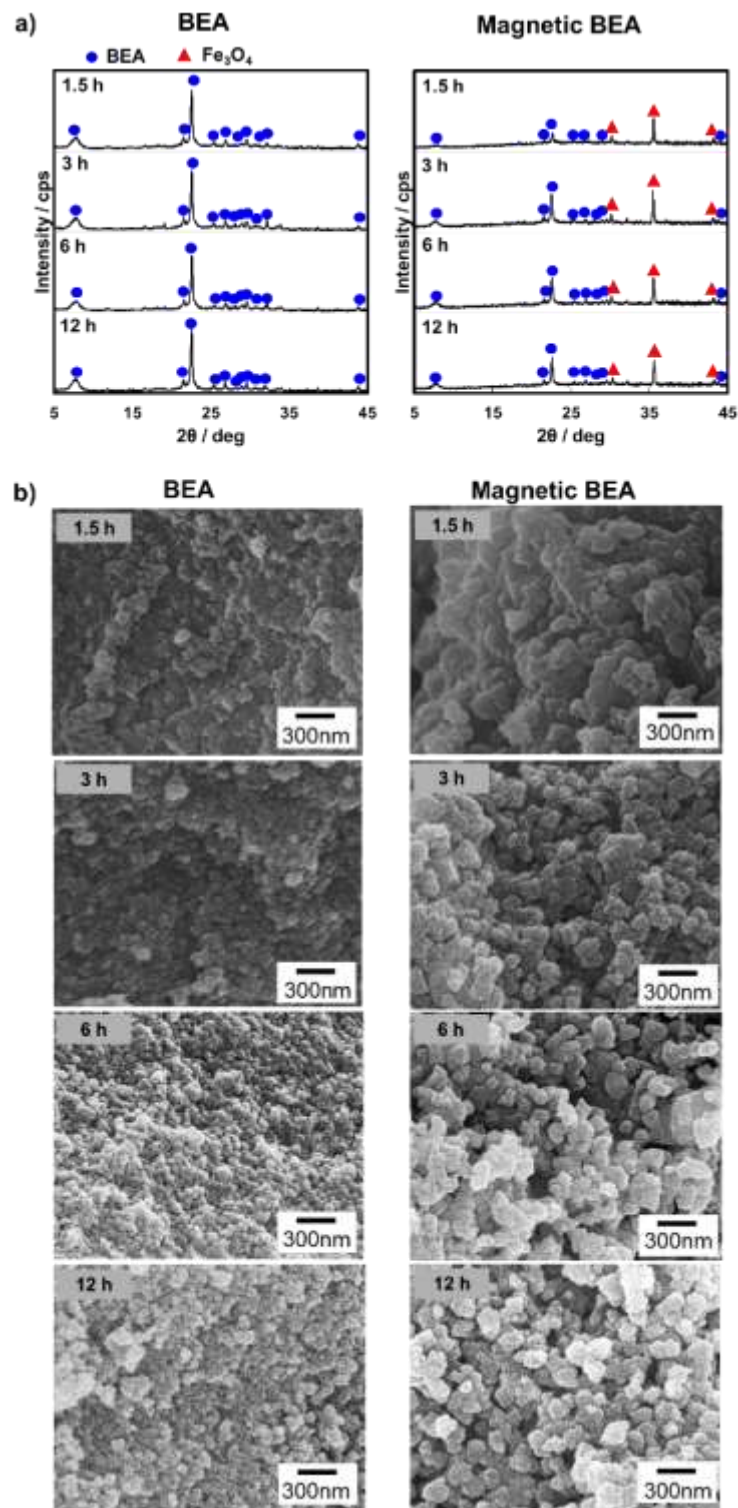


Fig. 4 Magnetization curves of **a)** magnetic BEA, denoted as MBEA, and **b)** BEA measured at room temperature in comparison with Fe_3O_4 . Numbers in the data series names represent calcination temperatures in $^\circ\text{C}$

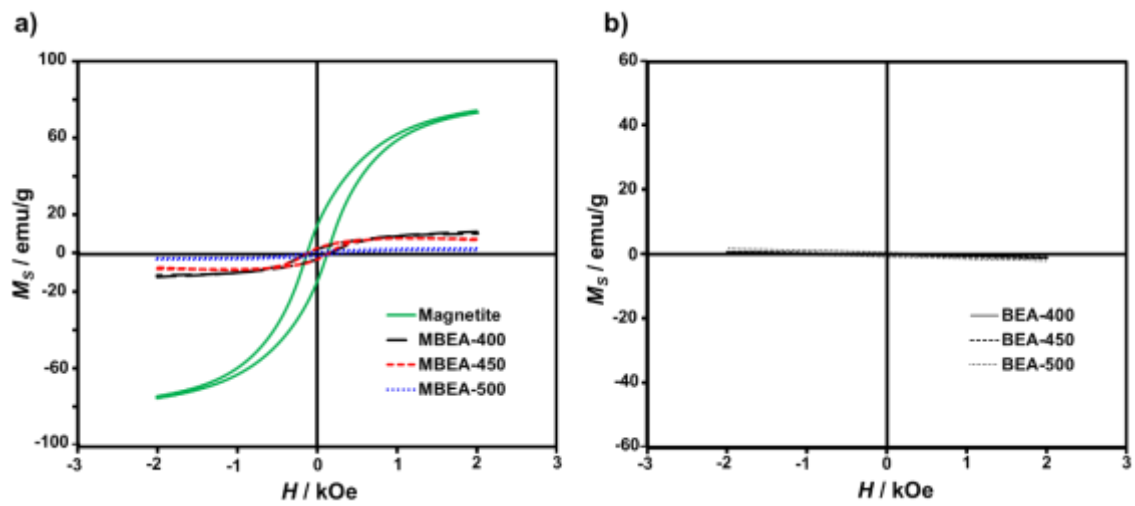


Fig. 5 Adsorption isotherm of sulfadiazine onto BEA and magnetic BEA-type zeolites calcined at 450°C

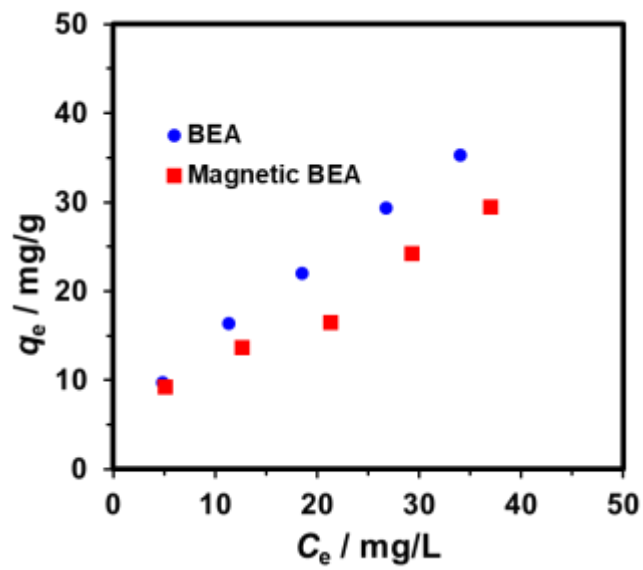


Fig. 6 Adsorption isotherm plots using Langmuir and Freundlich models of sulfadiazine onto BEA and

magnetic BEA-type zeolites calcined at 450 °C

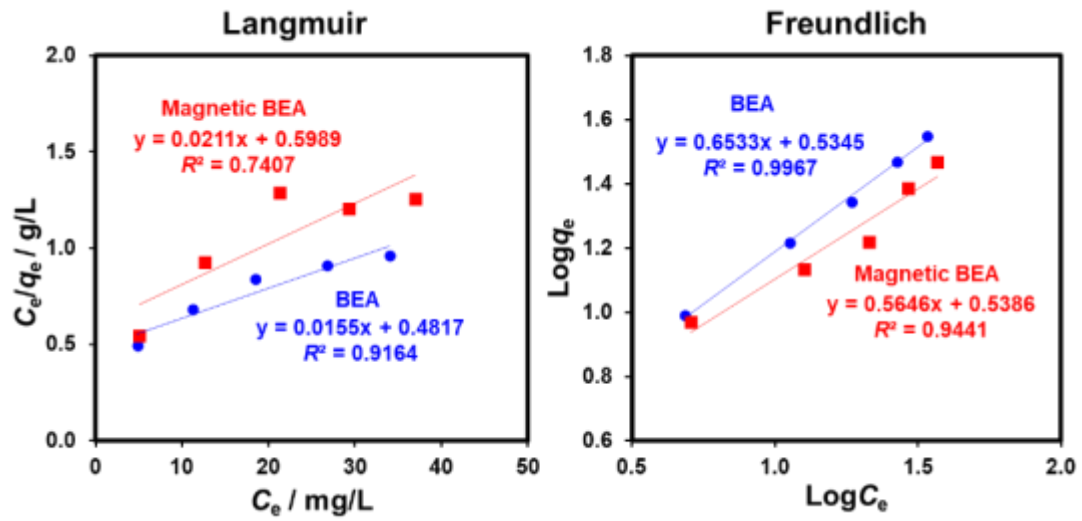


Fig. 7 Fraction species and adsorbed amount percentage of sulfadiazine on BEA (circle marker) and magnetic BEA (diamond marker) at different pH values. The adsorbed amount percentage was calculated as per total amount of sulfadiazine in the initial solutions (20 mg/L)

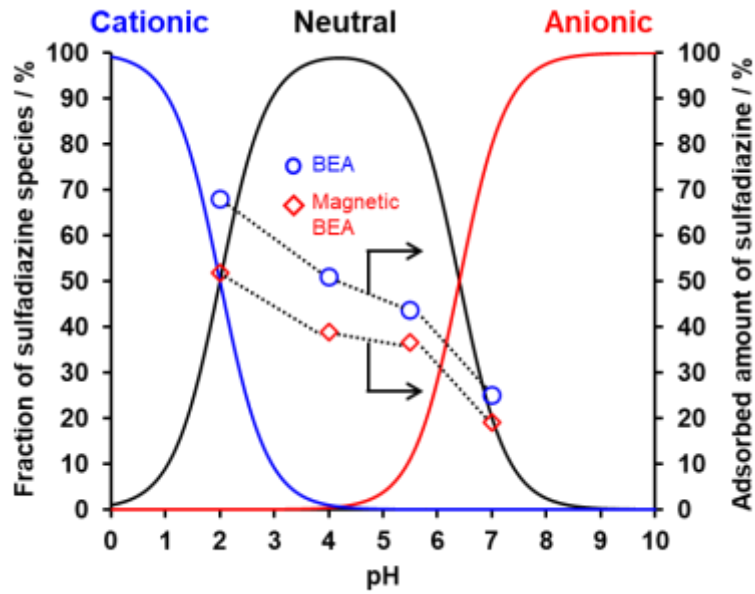


Fig. 8 Equilibrium amount of sulfadiazine adsorbed on BEA and magnetic BEA after each adsorption/regeneration cycle

